inter-noise 2007 istanbul

INTER-NOISE 2007

28-31 AUGUST 2007
ISTANBUL, TURKEY

Vibro-acoustic model of a geared system including friction excitation

Rajendra Singh*, Allison Lake, Vivake Asnani and Song He
Acoustics and Dynamics Laboratory
Department of Mechanical Engineering
The Ohio State University
Columbus, OH 43210, USA

*Corresponding Author: The Donald D. Glower Chair in Engineering and Professor
E-mail: <singh.3@osu.edu>
Phone: 614-292-9044
Fax: 614-292-3163

ABSTRACT

Semi-analytical vibro-acoustic models of a geared system are developed and experimentally validated to comparatively assess the effects of static transmission error and sliding friction excitations. An eight degree-of-freedom model incorporating the off-line-of-action direction is analytically formulated for a spur gear pair, in which the friction force excitation is assumed to act externally with given amplitude for all frequencies. Predicted dynamic bearing forces are examined in both the line-of-action and off-line-of-action directions. Noise levels are then calculated at the gear mesh harmonics, based on empirical structural-acoustic transfer functions that were determined by experiments on the Gear Noise Rig at NASA's Glenn Research Center. The predicted noise levels are compared to measurements collected in an anechoic chamber surrounding the test rig. The results exemplify the importance of modeling the friction excitation and off-line-of-action dynamics, but further development is required to yield quantitative noise predictions.

1 INTRODUCTION

Integrated models of a gearbox and its internal components are essential for accurate predictions of gear noise, and most studies on gearbox system dynamics relied on a combination of detailed finite element (FE), boundary element (BE) and semi-analytical methods. For example, Van Roosmalen [1] formulated a gearbox model including analytical formulations for gear vibrations due to tooth deflections and the bearing transfer path. Lim and Singh [2] developed both a lumped parameter model and a FE model with a flexible casing for a simple geared system. Kartik and Houser [3] used a FE model of a double-mesh geared system with spur gear pair that was utilized to predict the dynamic forces at the bearings. However, finite and boundary element methods often require much computational time for parametric studies. In such cases, simple models for the gearbox are more desirable [4]. It has been shown [3, 5] that the frequency response functions (FRFs) of the housing could be experimentally measured and incorporated into the modeling process.

Sliding friction in geared systems has been found [6-9] to have significant effect on the overall noise and vibration. Hence, there is a need for analytical models that incorporate the sliding friction into the system to examine the off-line-of-action (OLOA) dynamics. The objective of this research is to use the source-path-receiver concept of Fig. 1 to predict gear whine noise excited by both the static transmission error (STE) and sliding friction. These two excitations are inputs to a linear 8 degree-of-freedom (DOF) model, which is characterized by natural frequencies ω_r and mode shapes ϕ_r. This study focuses on the prediction of dynamic bearing forces in both the line-of-action (LOA) and OLOA directions. These forces are coupled at the bearings with housing structures which cause the out-of-plane vibrations of housing panels. The structural velocity of the housing is radiated as sound pressure, where it is perceived by the receiver. A simple model utilizing measured acoustic-structural transfer functions (pressure/acceleration p/a) is then employed to predict the sound pressure level (SPL) at the gear mesh harmonics. The transfer functions are measured on the NASA GRC Noise Rig for a unity-ratio spur gear pair system with parameters listed in Table 1. An order of magnitude comparison could thus be made to experimental data at selected mesh harmonic frequencies. Note that the same gear set and rig were used to generate the transfer functions and to collect the sound and vibration data. This should allow us to assess the relative importance of two gear noise sources of Fig. 1.

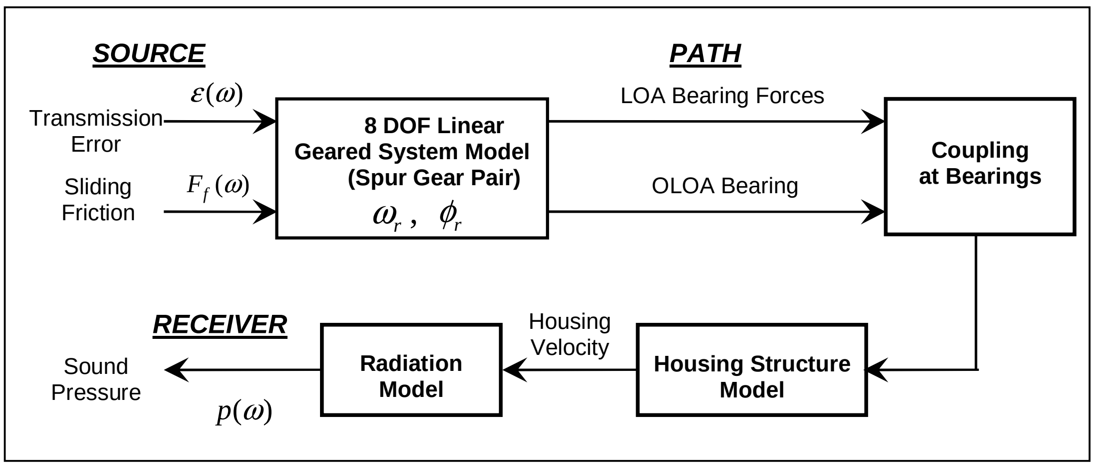

Figure 1: Conceptual description of the vibro-acoustics of a geared system with two excitations, given linear system assumption

Table 1: NASA spur gear set specifications

Pressure angle, deg	20	Number of teeth	28
Diametral pitch, in^{-1}	8	Center distance, in	3.5
Circular pitch, in	0.3927	Base diameter, in	3.2889
Outside diameter, in	3.738	Profile contact ratio	1.57
Face width, in	0.25	Moment of inertia, in-lb-s^2	3.22×10^{-3}
Gear mass, lb-s^2/in	1.8×10^{-3}	Shaft mass, lb-s^2/in	1.60×10^{-2}
Load (motor) inertia, in-lb-s^2	7.8 (3.5)	Gear mesh stiffness, lb/in	3.6×10^{5}
Torsional shaft stiffness, in-lb/rad	3.4×10^{5}	Effective bearing/shaft stiffness, lb/in	1.29×10^{5}

2 LINEAR SYSTEM MODEL WITH OFF-LINE-OF-ACTION (OLOA) DYNAMICS

2.1 Problem formulation of gear pair system

The schematic for the 8 DOF gear pair system is shown in Fig. 2. The pinion (subscript p)

and gear (subscript g) each has one vibratory angular motion θ as well as two translational motions x and y corresponding to the LOA and OLOA motions. The base radius and inertia are denoted by R and J with averaged mesh stiffness represented by k_m. Symbol m represents the mass of the pinion/gear along with contributions from the respective shafts. The inertias of the motor and load are denoted by J_d and J_L, and the torsional input and output shaft stiffness (viscous damping coefficients) are given as k_{Td} and k_{TL} (c_{Td} and c_{TL}). The input and output torques at the motor and load are T_d and T_L. Here, both shafts are modeled as simply supported beams with the effective shaft-bearing stiffness designated by k_x and k_y in the LOA and OLOA directions, respectively. The corresponding viscous damping coefficients of similar notation are also included.

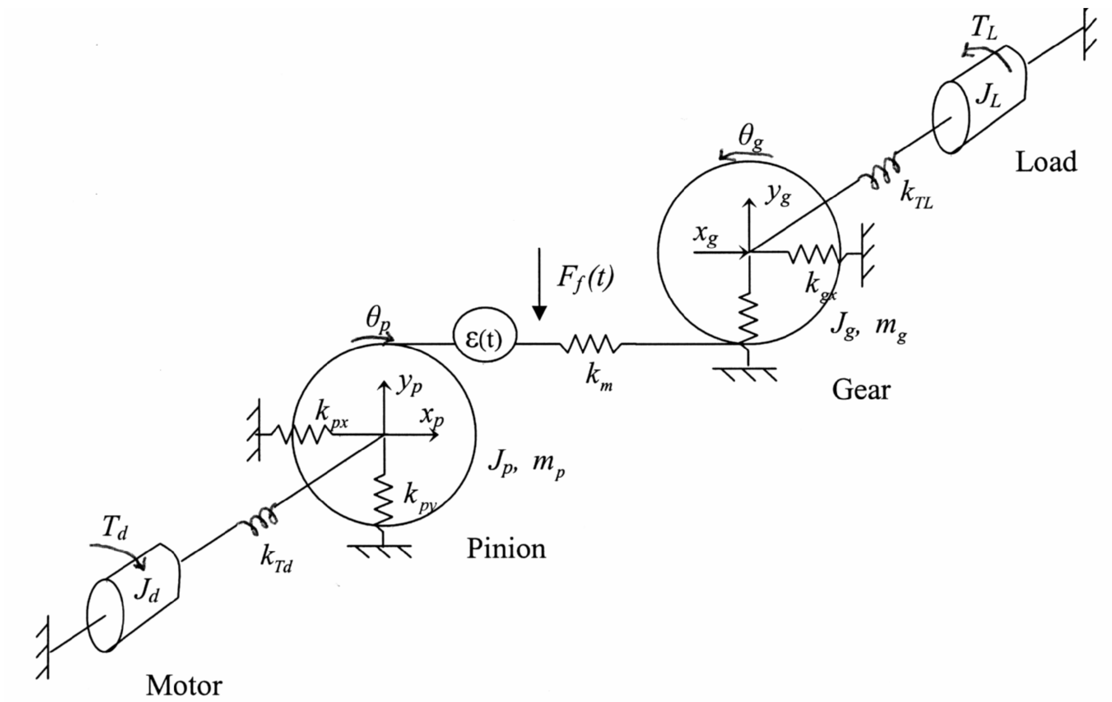

Figure 2: Schematic of the 8 DOF geared system with spur gear pair (damping elements not shown)

Besides the loaded STE displacement excitation $\varepsilon(t)$ at the gear mesh in the LOA direction, the friction force excitation $F_f(t)$ is assumed to act externally at gear mesh in the OLOA direction. For the example case of NASA gear pair (Table 1), assumed excitations have constant amplitudes over the entire frequency range. Also, averaged moment arm ξ of 0.6 in. is used for the calculation of the friction torque T_f. The governing equations of system in Fig. 2 are given as follows, where the viscous damping matrix $\underline{\underline{C}}$ is proportional to the stiffness matrix $\underline{\underline{K}}$ (by exchanging all k terms into corresponding c terms):

$$\underline{\underline{M}}\,\underline{\ddot{q}} + \underline{\underline{C}}\,\underline{\dot{q}} + \underline{\underline{K}}\,\underline{q}(t) = \underline{Q}(t) \tag{1a}$$

$$\underline{\underline{M}} = [diag(J_d, m_p, m_p, J_p, J_g, m_g, m_g, J_L)] \tag{1b}$$

$$
\underline{\underline{K}} = \begin{bmatrix}
k_{Td} & 0 & 0 & -k_{Td} & 0 & 0 & 0 & 0 \\
0 & k_{py} & 0 & 0 & 0 & 0 & 0 & 0 \\
0 & 0 & k_{px}+k_m & R_p k_m & -R_g k_m & -k_m & 0 & 0 \\
-k_{Td} & 0 & R_p k_m & R_p^2 k_m + k_{Td} & -R_p R_g k_m & -R_p k_m & 0 & 0 \\
0 & 0 & -R_g k_m & -R_p R_g k_m & R_g^2 k_m + k_{TL} & R_g k_m & 0 & -k_{TL} \\
0 & 0 & -k_m & -R_p k_m & R_g k_m & k_{gx}+k_m & 0 & 0 \\
0 & 0 & 0 & 0 & 0 & 0 & k_{gy} & 0 \\
0 & 0 & 0 & 0 & -k_{TL} & 0 & 0 & k_{TL}
\end{bmatrix} \qquad (1c)
$$

$$
\underline{q}(t) = \begin{bmatrix} \theta_d \\ y_p \\ x_p \\ \theta_p \\ \theta_g \\ x_g \\ y_g \\ \theta_L \end{bmatrix}, \qquad
\underline{Q}(t) = \begin{bmatrix} T_d(t) \\ -F_f(t) \\ c_m\dot{\varepsilon} + k_m\varepsilon(t) \\ \xi F_f(t) + c_m R_p\dot{\varepsilon} + k_m R_p \varepsilon(t) \\ -\xi F_f(t) - c_m R_g \dot{\varepsilon} - k_m R_g \varepsilon(t) \\ -c_m\dot{\varepsilon} - k_m\varepsilon(t) \\ F_f(t) \\ T_L(t) \end{bmatrix} \qquad (1e\text{-}d)
$$

2.2 Dynamic Bearing Forces in Two Directions

The dynamic bearing forces could be predicted by the linear system described in Eq. (1) and they are transmitted to excite the gearbox housing. Figure 3 compares the effect of variation in μ on both the LOA and OLOA dynamics. A baseline spectrum corresponding to μ = 0.001 is plotted corresponding to an ideal case negligible friction. Likewise, μ = 0.04 represents the case where the friction force and STE force are of similar magnitude (13 lb.) and μ = 0.1 is the case with high friction force (33.5 lb.) as compared to the STE force. The same STE input of 42 μ-in is assumed in the LOA direction. Observe in Fig. 3(a) that an increase in μ results in larger bearing forces across the frequency range away from the resonances. Below the first resonance, the force increases at the same rate as the increase in μ. Such effect, however, is not as significant over the higher frequency range, say beyond resonance at 4345 Hz. The variation in μ has moderate influence on the resonant peaks, especially at the lower frequencies. Next, the OLOA bearing force is examined in Fig. 3(b) where only one single mode is present at 429 Hz. The slope of the response below the resonance is zero, where the bearing force is equal to the magnitude of the assumed friction input, and the spectrum decreases at a rate of 40 dB/decade beyond the resonance. An increase in μ results in a proportional increase in bearing force across the entire frequency range including the resonance.

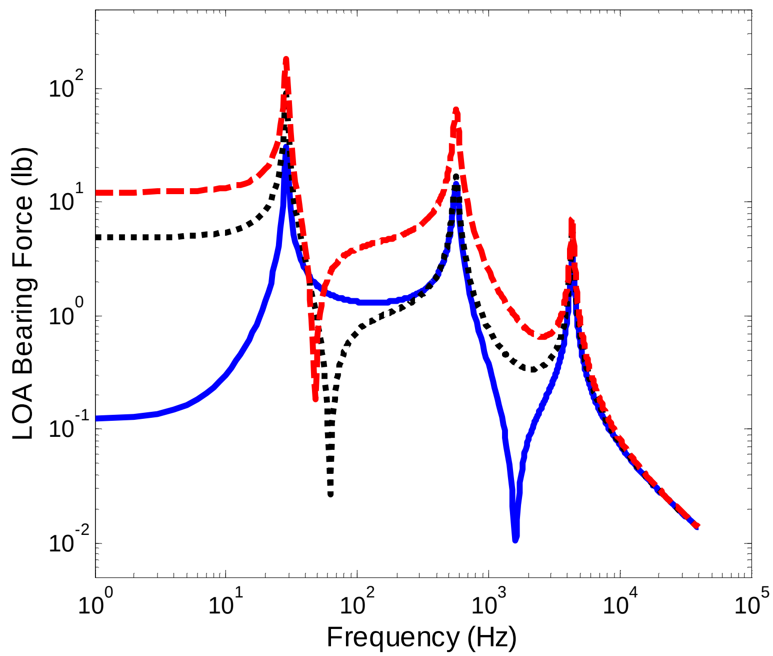

(a)

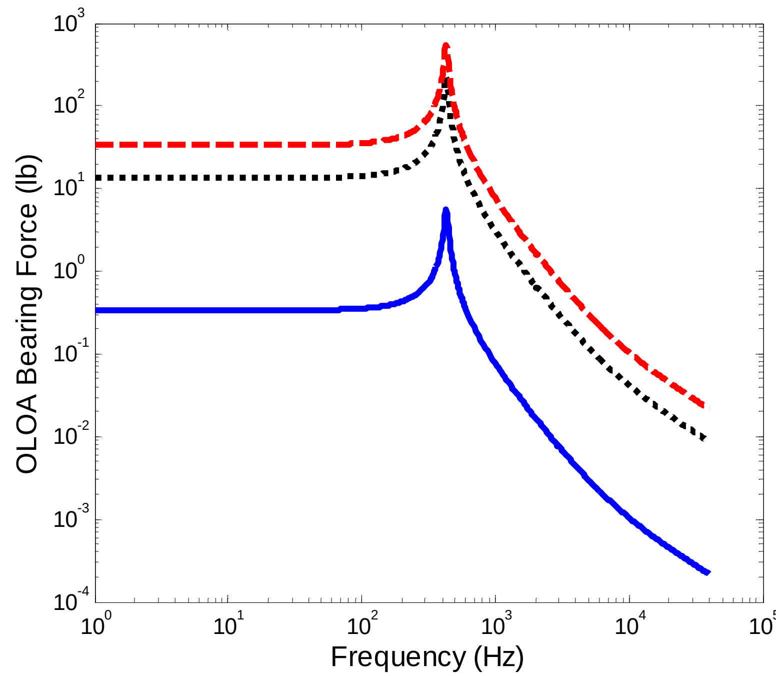

(b)

Figure 3: Effect of the friction coefficient (μ) on the dynamic bearing forces (a) in the LOA direction; (b) in the OLOA direction. Key: ———, μ = 0.001; ------- μ = 0.04; – – – –, μ = 0.1.

2.3 Prediction of Gearbox Noise

In terms of the source-path-receiver concepts of Fig. 1, predictions of dynamic bearing forces provide structure-borne excitations to the gearbox housing, which could significantly amplify the transmitted vibrations and noise since the panels are efficient radiators. By relating the dynamic bearing forces to measured sound pressure levels (SPL), predictions can be directly compared with experimental data. The LOA and OLOA accelerations at the mesh harmonic frequencies are combinations of the accelerations due to translational and rotational motions; they could be derived as follows where $\omega = m\ \omega_m$ in which m is the gear mesh harmonic index.

$$a_x(\omega) = \ddot{x}_g + R_g\ddot{\theta}_g\,, \qquad a_y(\omega) = \ddot{y}_g \tag{2a,b}$$

These dynamic responses, along with the transfer functions measured in both the LOA and OLOA directions, could provide the sound pressure at the gear mesh frequencies:

$$p_x(\omega) = H_x a_x(\omega)\,, \quad p_y(\omega) = H_y a_y(\omega)\,, \tag{3a,b}$$

Here, H_x and H_y (in the units of μPa/(in/s^2)) are the acoustic-structural (p/a) transfer functions measured in the LOA and OLOA directions, in which a is the translational gear acceleration (in/s^2). Although the phase of the sound pressures in the two directions is unknown, a maximum and minimum could be determined by assuming an in-phase and out-of-phase relationship, respectively. Thus, a range of possible values could be predicted, such that $p_{min} \le p(\omega) \le p_{max}$, where

$$p_{max} = p_x + p_y\,, \qquad p_{min} = p_x - p_y\,. \tag{4a,b}$$

However, prediction results are only given in terms of the maximum values due to the space limitation. The sound pressure is converted into unweighted dB scale using 20 μPa as reference. The LOA and OLOA gear accelerations are calculated at the mesh harmonics assuming realistic forces predicted by *LDP* [10]. The sound pressures are determined for the range of mean loads from 500 to 900 in-lb.

3 MEASUREMENT BASED GEAR NOISE PATH CONTRIBUTION STUDY

Several structural-borne noise transmission paths (transfer functions) were measured on the NASA GRC (parallel axis) Gear Noise Rig based on the assumption that the quasi-static system response is similar to the response under rotating conditions, since the torque was expected to only affect the gear mesh resonances. The gearbox was modified to allow controlled excitations to be applied to the gear-mesh and measured. Brackets were welded to the bedplate of the gear-rig to mount shakers in the LOA and OLOA directions outside the gearbox, as shown in Fig. 4(a). Stinger rods were connected from the shakers through two small holes in the gearbox and attached to a machined collar, which was secured to the input shaft. The collar allowed the stingers to be aligned at the center of the shaft, so no torsion was produced by the translational excitations. Furthermore, the collar fit around the shaft without clearance to prevent backlash. The gear-pair was locked in single tooth contact and a small aluminum block was adhered just behind the loaded tooth of the gear. Two mini accelerometers were fastened to the block to measure the LOA and OLOA mesh accelerations resulting from shaker excitation. The total mass of the accelerometers and aluminum block was insignificant compared to the gear-blank, so mass loading was not a concern. Experiments were done with only one shaker activated at a time with a 600 lb-in static preload. The load was chosen based on coherence measurement between the shaker input voltages and measured gear-tooth accelerations. Torque was increased until the fidelity deteriorated (as indicated by the coherence) and then backed off significantly. An anechoic sound measurement enclosure was built to isolate the gearbox and mitigate reflected sound, as shown in Fig. 4(b).

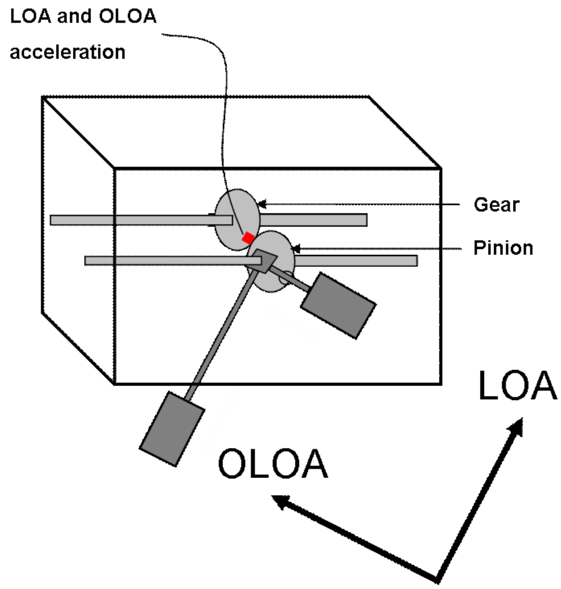

(a)

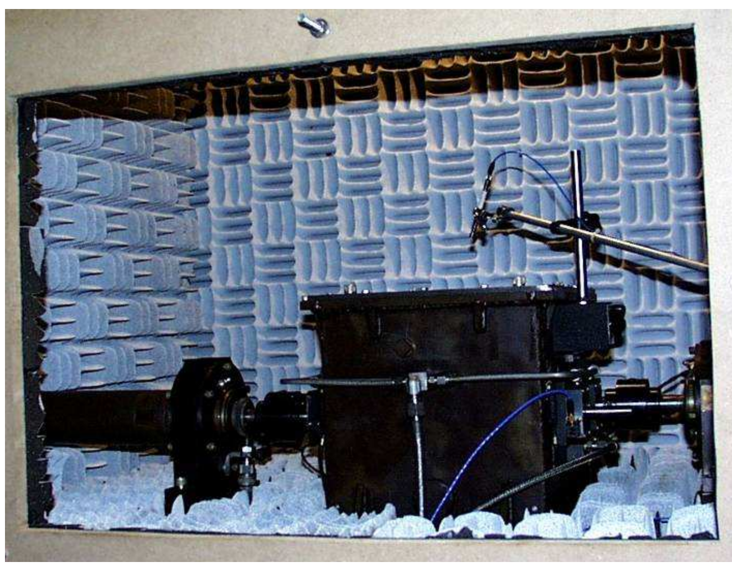

(b)

Figure 4: (a) Mesh excitations in the LOA and OLOA directions using external shakers. (b): View through front access door of the dedicated anechoic chamber

To excite the system, band-limited random noise signals were amplified and then applied to either the LOA or OLOA shaker. The resulting vibration or sound was observed with several accelerometers and microphones. These data was manipulated in the frequency domain to generate the vibro-acoustic transfer functions. The data processing steps are explained in [14]. Figure 5 shows an example of H_x obtained from the LOA acceleration at the gear teeth to the microphone located 6 in. from the top gearbox plate. The H_y spectrum in the OLOA direction is similar. It is clear that numerous gear dynamic and housing structural modes exist across the frequency spectrum while the sound pressure levels (SPL) are predicted only at the gear mesh harmonics (m) to represent the realistic excitation.

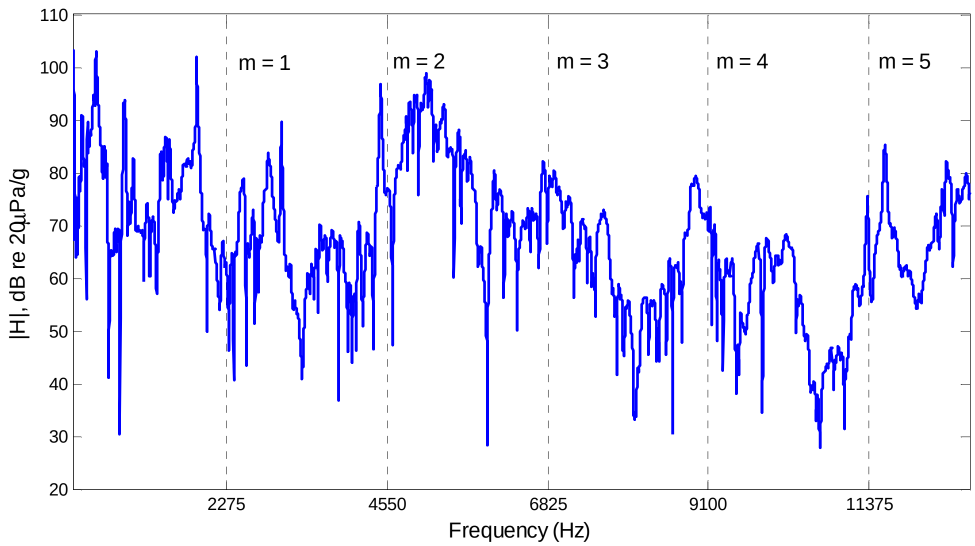

Figure 5: Measured transfer function (*p*/*a*) from the LOA acceleration: (a) of the gear teeth to the microphone (p) located 6 inches above the top plate of the gearbox. The speed was chosen so that mesh harmonics (*m*: mesh index) exited non-resonant frequencies, at positions where the transfer function magnitude was relatively high.

As conceptually shown by the block diagram in Fig. 1, this measured transfer function is essentially a combination of several gear dynamic, housing structural and radiation transfer functions within the system.

$$\frac{p}{a_g} = \left(\frac{p}{a_h}\right)\left(\frac{a_h}{F_{br\_ext}}\right)\left(\frac{F_{br\_ext}}{F_{br\_int}}\right)\left(\frac{F_{br\_int}}{a_g}\right) \tag{5}$$

Here, F_{br_int} / a_g is the bearing force/gear acceleration transfer function and F_{br_ext} / F_{br_int} represents the coupling at the bearings which relates the internal forces to the external forces. The latter transfer function (force transmissibility across the bearings in a multi-dimensional manner) could not be directly measured. The external forces excite the gearbox housing structural acceleration through a_h / F_{br_ext} and then radiated as sound pressure from the radiating surfaces, defined by the p/a_h transfer function.

4 COMPARISON OF GEAR NOISE PREDICTION WITH MEASUREMENT

The Gear Noise Rig at NASA Glenn was operated with the unity ratio spur gear set described in Table 1. Vibro-acoustic responses were measured at various microphone locations within the NASA gearbox. In the experiment, the mean torque was varied over the range from 500 to 900 in-lb. at a speed of 4875 Hz. This particular speed created gear mesh harmonics that corresponded to the highest coherence values in the measured transfer functions of the rig. While several vibration and sound measurements were taken, only the noise data obtained at 6 in. above the top-plate are shown here. The oil temperature was also varied in these experiments, and the case of 140 °F (60°C) (measured for the oil flinging-off the gears as they enter into mesh) is utilized for comparison.

Utilizing Eqs. (1)-(4), a predicted range of SPLs was determined for each of the gear mesh harmonics. The predicted results were normalized with respect to the maximum pressure (μPa) occurring at the 2nd mesh harmonic and a mean load of 900 in-lb. The comparison presented here is only on an order of magnitude basis. Note the measured transfer functions may contain errors; further, we may not have accurately modeled all of the parameters. Figure 6 shows the normalized amplitudes for the first four mesh harmonics across the range of loads. Sound level of 1st harmonic is expected to increase as the load increases since tip relief is applied with a "optimal" load of 600 in-lb, however, the measured data shows the opposite, which has a relative minimum at 800 in-lb. while the maximum amplitude corresponds to a load of 500 in-lb. It is possible that the airborne source is affecting the measurement at this mesh harmonic, while the experimental study focused only on measuring the structure-borne noise [11]. The spectra of the 2nd mesh harmonic show similar behavior with increases in load. Both the prediction and measurement have maximum SPL at the 2nd mesh harmonic. In fact, the rest of the harmonics all generally show an increasing trend versus load. The predicted SPL harmonics seem to increase somewhat linearly with torque. Also, prediction shows a significant amplitude for the 3rd harmonic, which is greater than the 1st harmonic. However, SPL measurements show the 1st harmonic is more significant. Definitive conclusions could not be drawn based on the limited results and a lack of accurate system parameters. Nevertheless, the implementation of the proposed noise prediction model highlights a key area for improvement over the existing literature, and thus it should be pursued in future research.

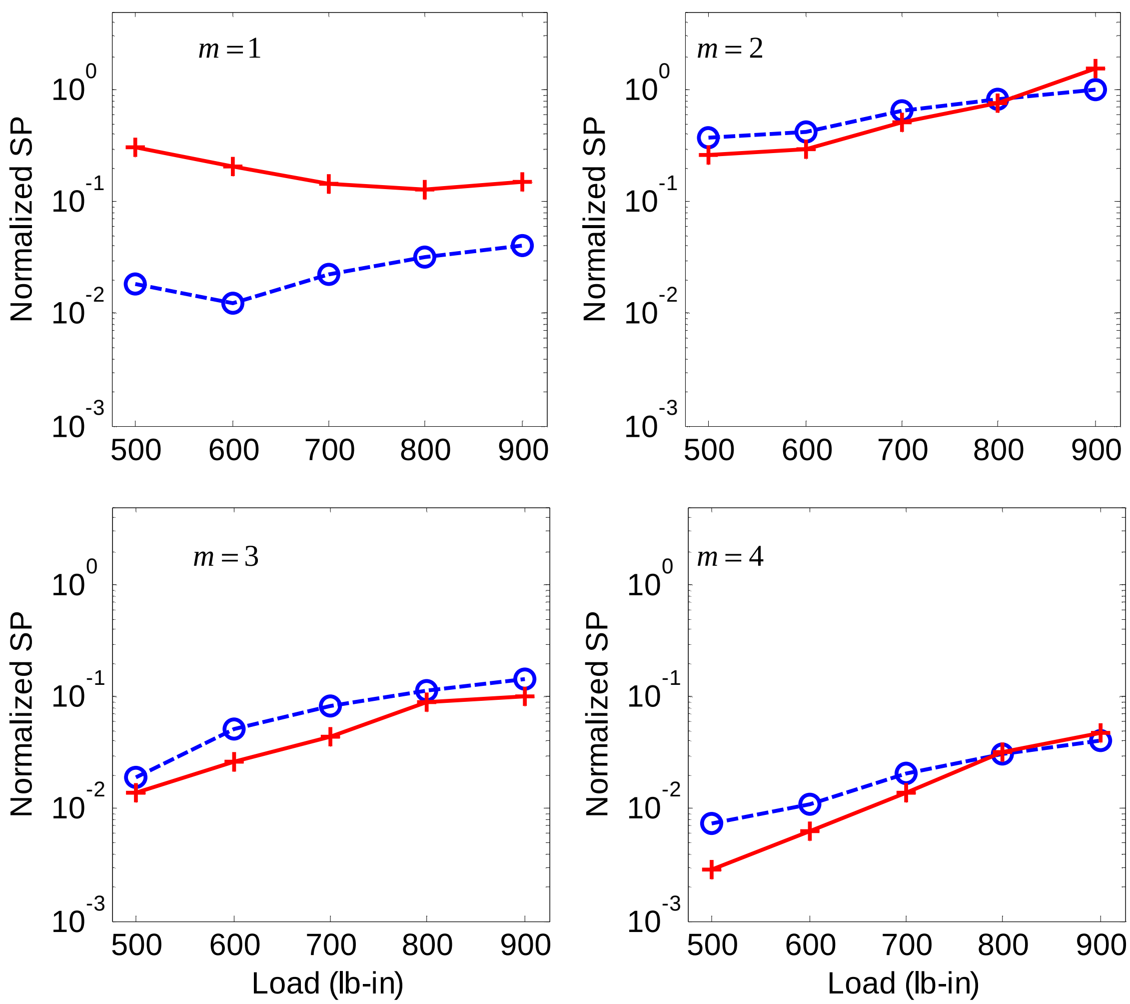

Figure 6: Comparison of the normalized sound pressure level predictions with measurements at the first four gear mesh harmonics (m = 1, 2, 3, 4). Key: —+—, measurements; –⊖– predictions.

5 CONCLUSION

A linear model of the internal geared system has been developed to examine the OLOA vibration due to the friction excitation in addition to the STE excitation in frequency domain. A comparison of the bearing force spectra showed that the friction force dictates the OLOA dynamics and it also significantly influences the maximum force in the LOA direction. This indicates the importance of including friction effects in the vibration analysis. A method was presented to predict the radiated SPL using an experimental transfer function and realistic excitations, at the gear mesh harmonics. The results showed maximum SPL at the 2nd mesh harmonic while the 3rd harmonic was much higher than the 1st. The proposed noise prediction method should be expanded further. For instance, both air-borne and structure-borne noise issues, as excited by surface finish should be considered.

6 ACKNOWLEDGEMENTS

This article is based upon a three-year study that was supported by the U. S. Army Research Laboratory and the U. S. Army Research Office under grant number DAAD19-02-1-0334. We thank NASA GRC for providing us experimental facilities. We acknowledge Prof. G. Pavic (INSA Lyon, France) for his support for the last author.

7 REFERENCES

[1] Van Roosmalen, A., 1994, "Design Tools for Low Noise Gear Transmissions," Ph. D. Dissertation, Eindhoven University of Technology.

[2] Lim, T.C. and Singh, R., 1991, "Vibration Transmission Through Rolling Element Bearings. Part III: Geared Rotor System Studies," *Journal of Sound and* Vibration, **151**(1), pp. 31-54.

[3] Kartik, V. and Houser, D. R., 2003, "An Investigation of Shaft Dynamic Effects on Gear Vibration and Noise Excitations," *SAE* Paper #2003-01-1491.

[4] Steyer, G., 1987, "Influence of Gear Train Dynamics on Gear Noise," *NOISE-CON 87*, pp. 53-58.

[5] Oswald, F., Seybert, A., Wu, T. and Atherton, W., 1992, "Comparison of Analysis and Experiment for Gearbox Noise," *Proceedings of the International Power Transmission and Gearing Conference*, Phoenix, pp. 675-679.

[6] Rebbechi, B., Oswald, F. and Townsend, D., 1996, "Measurement of Gear Tooth Dynamic Friction," *NASA Technical Memorandum* 107279.

[7] Houser, D., Vaishya, M. and Sorenson, J., 2001, "Vibro-Acoustic Effects of Friction in Gears: An Experimental Investigation," *SAE* Paper #2001-01-1516.

[8] Vaishya, M., and Singh, R., 2003, "Strategies for Modeling Friction in Gear Dynamics," ASME J. Mech. Des., **125**, pp. 383-393.

[9] He, S., Gunda, R., and Singh, R., 2007, "Effect of Sliding Friction on the Dynamics of Spur Gear Pair with Realistic Time-Varying Stiffness," J. Sound Vib., **301**, pp. 927-949.

[10] *Load Distribution Program,* Gearlab – The Ohio State University, 2005.

[11] Rook, T. and Singh, R., 1996, "Mobility analysis of structure-borne noise power flow through bearings in gearbox-like structures," *Noise Control Engineering Journal*, **44**(2), pp. 69-78

[12] Rebbechi, B., Oswald, F. and Townsend, D., 1991, "Dynamic Measurements of Gear Tooth Friction and Load," *NASA Technical Memorandum* 103281.

[13] Houser, D. and Ozguven, H., 1988, "Mathematical Models used in Gear Dynamics - A Review," *Journal of Sound and Vibration*, **121**(3), pp.383-411.

[14] Singh, R., 2005, "Dynamic Analysis of Sliding Friction in Rotorcraft Geared Systems," technical report submitted to the Army Research Office, grant number DAAD19-02-1-0334.